

Short
CommunicationSubcellular localization of the severe acute
respiratory syndrome coronavirus nucleocapsid
proteinJaehwan You,¹ Brian K. Dove,¹ Luis Enjuanes,² Marta L. DeDiego,²
Enrique Alvarez,² Gareth Howell,³ Paul Heinen,^{4†} Maria Zambon⁴
and Julian A. Hiscox^{1,3}

Correspondence

Julian A. Hiscox
j.a.hiscox@leeds.ac.uk¹Institute of Molecular and Cellular Biology, Faculty of Biological Sciences, Garstang Building,
University of Leeds, Leeds LS2 9JT, UK²Department of Molecular and Cell Biology, Centro Nacional de Biotecnología (CNB, CSIC),
Campus Univ. Autónoma, 3 Darwin Street, Cantoblanco, 28049 Madrid, Spain³Astbury Centre for Structural Molecular Biology, University of Leeds, Leeds LS2 9JT, UK⁴Health Protection Agency, London NW9 5HT, UK

The coronavirus nucleocapsid (N) protein is a viral RNA-binding protein with multiple functions in terms of virus replication and modulating cell signalling pathways. N protein is composed of three distinct regions containing RNA-binding motif(s), and appropriate signals for modulating cell signalling. The subcellular localization of severe acute respiratory syndrome coronavirus (SARS-CoV) N protein was studied. In infected cells, SARS-CoV N protein localized exclusively to the cytoplasm. In contrast to the avian coronavirus N protein, overexpressed SARS-CoV N protein remained principally localized to the cytoplasm, with very few cells exhibiting nucleolar localization. Bioinformatic analysis and deletion mutagenesis coupled to confocal microscopy and live-cell imaging, revealed that SARS-CoV N protein regions I and III contained nuclear localization signals and region II contained a nucleolar retention signal. However, cytoplasmic localization was directed by region III and was the dominant localization signal in the protein.

Received 1 April 2005

Accepted 4 September 2005

Severe acute respiratory disease coronavirus (SARS-CoV) is a nidovirus. One of the most abundant viral proteins produced inside a coronavirus-infected cell is the nucleocapsid (N) protein, a multifunctional phosphoprotein (Calvo *et al.*, 2005; Chen *et al.*, 2005; Jayaram *et al.*, 2005), which can bind viral RNA with high affinity (Chen *et al.*, 2005) to form a ribonucleocapsid structure (Risco *et al.*, 1996). SARS-CoV N protein (SARS-CoV-N) can also regulate cellular processes (He *et al.*, 2003; Luo *et al.*, 2005; Surjit *et al.*, 2004). Based on amino acid sequence comparisons, three conserved regions have been identified in the coronavirus N protein (Parker & Masters, 1990), which may serve as RNA-binding sites and be involved in modulating cell signalling.

Coronavirus and the closely related arterivirus N proteins can localize to the cytoplasm, the nucleus and the nucleolus (Hiscox *et al.*, 2001; Ning *et al.*, 2003; Rowland *et al.*, 1999; Tijms *et al.*, 2002; Wurm *et al.*, 2001), and can bind/interact with nucleolar proteins (Chen *et al.*, 2002; Yoo *et al.*, 2003). The nucleolus is a dynamic subnuclear structure that is involved in ribosome subunit biogenesis and in the control

of cell growth (Andersen *et al.*, 2005; Lam *et al.*, 2005). Morphologically, the nucleolus can be divided into a fibrillar centre (FC), a dense fibrillar component (DFC) and an outer granular component (GC) (Thiry & Lafontaine, 2005). Whilst nucleolar localization of N protein has been described for arterivirus and coronaviruses, the potential nuclear/nucleolar localization of the SARS-CoV-N is unknown. The cellular localization of SARS-CoV-N may inform us to its potential function in modulating cell processes.

To investigate the distribution of SARS-CoV-N in the context of virus infection, Vero cells were infected with SARS-CoV with an m.o.i. of 0.5 in a P3 facility following EU biosafety regulations, and fixed at 16, 24, 48 and 72 h post-infection (p.i.) using 8% paraformaldehyde for analysis by indirect immunofluorescence with a rabbit polyclonal serum specific for SARS-CoV-N coupled with an Alexa 488-conjugated anti-rabbit immunoglobulin G. The nucleus was stained with ToPro3 (Molecular Probes). The experiment was repeated four times and representative images are shown in Fig. 1(a). The reason for choosing the later time points was that Qinfen *et al.* (2004) reported virus-like particles in the nucleus of Vero E6 cells infected with SARS-CoV at 72 h p.i. Our study indicated that whilst N protein

†Present address: Institute for Animal Health, Pirbright GU24 0NF, UK.

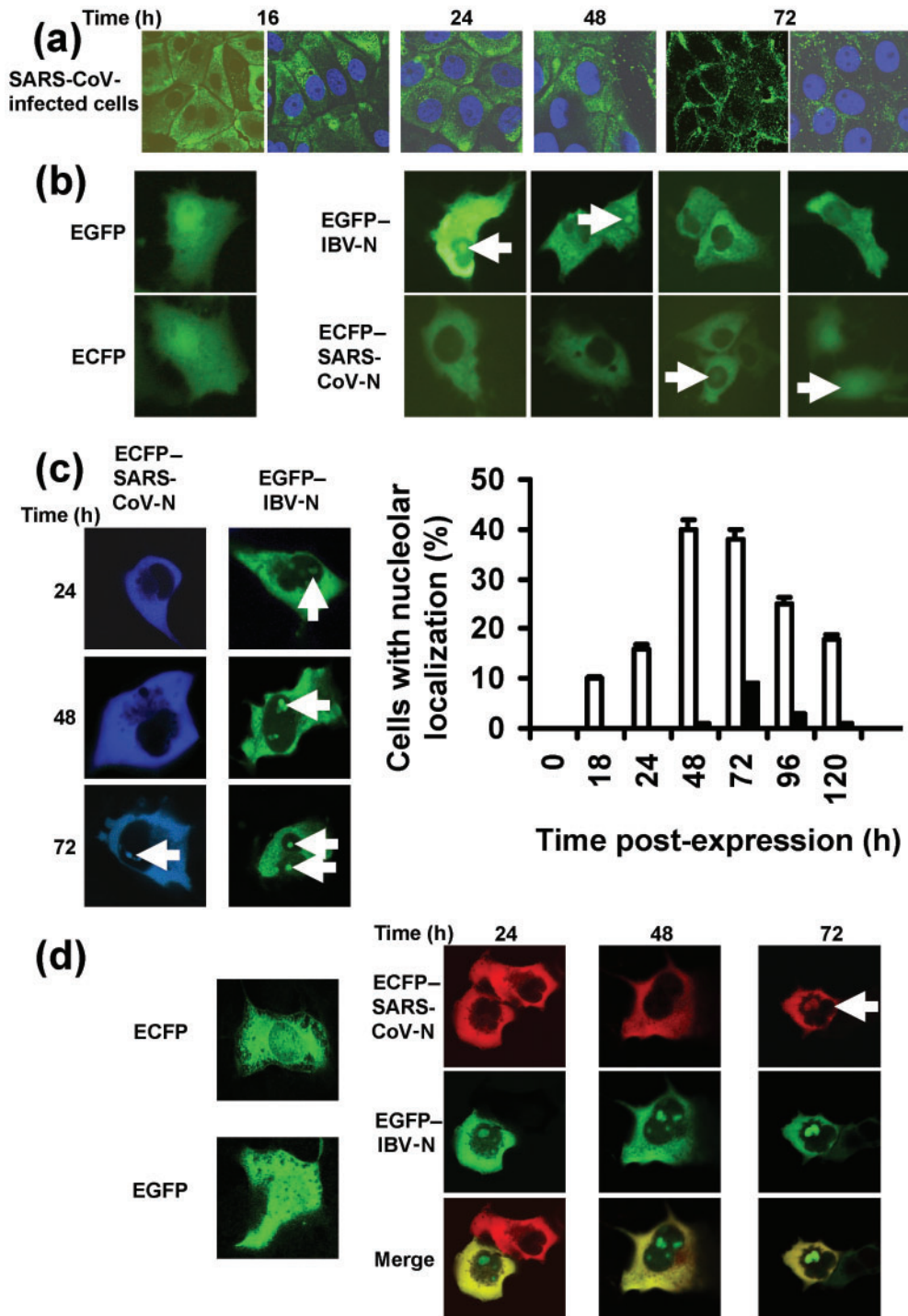


Fig. 1. (a) Confocal microscopy of the localization of SARS-CoV-N (green) at 16, 24, 48 and 72 h in cells infected with SARS-CoV, the nucleus is stained blue. For comparison, examples are also given for 16 and 72 h time points without staining of the nucleus. (b) Live-cell imaging of cells expressing EGFP, ECFP, EGFP-IBV-N or ECFP-SARS-CoV-N, several representative examples of the latter two are shown. Nucleoli are indicated by arrows. (c) Confocal microscopy of cells expressing either EGFP-IBV-N (green) or ECFP-SARS-CoV-N (blue) at 24, 48 and 72 h post-transfection. Nucleoli are indicated by arrows. Histogram of the percentage of cells expressing either EGFP-IBV-N (empty column) or ECFP-SARS-CoV-N (filled column), which exhibit cytoplasmic and nucleolar localization. The data are derived from 10 fields of view taken from three replicate experiments. (d) Confocal microscopy of cells expressing either EGFP (green) or ECFP (green) and cells transfected with both pECFP-SARS-CoV-N (false colour red) and pEGFP-IBV-CoV-N (green) at 24, 48 and 72 h post-transfection. Co-localization, where it occurs, is shown in yellow and nucleolus is indicated by an arrow.

localized to the cytoplasm at all time points, no nuclear or nucleolar localization was observed. Given the low m.o.i. used, the infection was not synchronised, and the earlier time point of 16 h p.i. may represent cells infected between 16 and 10 h p.i. (this latter time point due to cells being infected by progeny virus of the first round of infection).

Whilst no nucleolar localization of SARS-CoV-N was observed in infected cells, the successful detection of nucleolar proteins using antibodies can be related to the concentration of the protein within the nucleolus (Sheval *et al.*, 2005), in that the nucleolus is not always refractive to antibody staining. In addition, charged proteins can also migrate through cells post-fixation and become localized to the nucleus (Lundberg & Johansson, 2001, 2002). To address these concerns, and to investigate the subcellular localization of SARS-CoV-N in more detail, we generated vectors that expressed the protein (or parts of the protein) as a fusion with either enhanced cyan or green fluorescent protein (ECFP or EGFP, respectively). The protein could then be detected by direct fluorescence using both live-cell and confocal microscopy. As a control, we compared the subcellular localization of SARS-CoV-N with *Infectious bronchitis virus* N protein (IBV-N), which was located in either the cytoplasm alone or the cytoplasm and nucleolus (Hiscox *et al.*, 2001).

SARS-CoV N gene was cloned downstream of ECFP (vector pECFPC1; Clontech), creating pECFP-SARS-CoV-N, and IBV N gene was cloned downstream of EGFP (vector pEGFPC2; Clontech), creating pEGFP-IBV-N, and when expressed in cells, resulted in fluorescent fusion proteins ECFP-SARS-CoV-N and EGFP-IBV-N, respectively. To examine the subcellular localization of SARS-CoV-N, pECFP-SARS-CoV-N and pEGFP-IBV-N were transfected (using Lipofectin) into either Vero or Cos-7 cells, and subcellular localization was followed using live-cell imaging at 24 h post-transfection. As a control, cells were transfected with vectors expressing either ECFP or EGFP alone (pECFPC1 and pEGFPC2, respectively). The data indicated that whilst ECFP and EGFP localized predominately to the cytoplasm and the nucleus, the majority of ECFP-SARS-CoV-N localized to the cytoplasm, but, in a few cases, also to apparent subnuclear structures and the nucleus, whereas EGFP-IBV-N localized to either the cytoplasm or the cytoplasm and nucleolus (Fig. 1b). No difference in localization of either protein was observed between Vero and Cos-7 cells (data not shown), and therefore for subsequent analysis we used Cos-7 cells, as transfection was more efficient in this cell type. Similarly, in line with our previous results the position of a fluorescent tag at either the N terminus (in this present study) or C terminus of N protein did not affect localization of the fusion protein when compared to native protein (Hiscox *et al.*, 2001; data not shown).

The number of cells exhibiting nucleolar localization with ECFP-SARS-CoV-N appeared significantly less in comparison to EGFP-IBV-N. Therefore, we examined the subcellular localization of ECFP-SARS-CoV-N with

EGFP-IBV-N over a 120 h period. Cells were transfected with either pECFP-SARS-CoV-N or pEGFP-IBV-N. In order to accurately determine the distribution of both proteins, cells were fixed at each time point and visualized using confocal microscopy. Representative confocal images for the viral proteins are shown in Fig. 1(c) for 24, 48 and 72 h post-transfection. EGFP-IBV-N localized to either the cytoplasm alone or the cytoplasm and nucleolus, with a maximum of 40 % of transfected cells exhibiting this phenotype at 48 h. In contrast, ECFP-SARS-CoV-N localized predominately to the cytoplasm alone with a maximum of 10 % of transfected cells, showing both cytoplasm and nucleolar localization at 72 h post-transfection. Localization of proteins to the nucleolus at this time point could be an artefact, in that the cells have undergone several rounds of division and nuclear and nucleolar assembly. No difference was observed in the subcellular localization of both coronavirus N proteins using either live-cell imaging or fixing cells and visualizing using confocal microscopy. Therefore, this latter technique could be used to determine subcellular localization of the N protein in combination with marker proteins.

One hypothesis to account for the difference in nucleolar localization was that ECFP-SARS-CoV-N prevented entry or retarded entry of proteins into the nucleus. For example, a number of RNA viruses that replicate in the cytoplasm can alter the nuclear pore complex to prevent either import and/or export of proteins and RNAs to the nucleus (Gustin, 2003; Gustin & Sarnow, 2001, 2002). To investigate this, we co-transfected cells with pECFP-SARS-CoV-N and pEGFP-IBV-N, cells were then fixed at 24, 48 and 72 h, and the subcellular localization of these fusion proteins was examined using a Zeiss LSM510 Meta confocal microscope such that the ECFP signal was unmixed from the EGFP signal. Representative cells are shown in Fig. 1(d) (note that in dual-transfected cells ECFP has been falsely coloured red). The data indicated that in dual-transfected cells, EGFP-IBV-N localized to the cytoplasm and nucleolus with the same frequency as in singly transfected cells (data not shown), and that ECFP-SARS-CoV-N did not prevent the entry of a similar protein into the nucleus.

Another possibility to account for the difference in subcellular distribution between IBV-N and SARS-CoV-N was that ECFP-SARS-CoV-N disrupted nucleolar architecture, therefore preventing or reducing its own localization to the nucleolus. A number of viruses and viral proteins can disrupt nucleolar architecture (Hiscox, 2002, 2003), including IBV-N, although this did not prevent IBV-N from localizing to the nucleolus (Chen *et al.*, 2002). In addition, the previous experiment indicated that SARS-CoV-N did not inhibit localization of IBV-N. However, to investigate this possibility in more detail we examined cells that expressed ECFP-SARS-CoV-N by using confocal microscopy. Different nucleolar regions can be dissected using a combination of nucleolar marker proteins and appropriate fluorescent tag. B23 (DS-red) and nucleolin (EGFP) can be used to distinguish the FC and DFC, and EGFP-fibrillarin

can be used to distinguish the GC (Fig. 2a). In addition, phase-contrast microscopy can be used to visualize the FC, as this appears less refractive than the surrounding nucleolar regions (Fig. 2a).

Cells were co-transfected with pECFP-SARS-CoV-N and vectors that direct the expression of EGFP–nucleolin, EGFP–fibrillarin and DS-red-B23. The confocal microscope was used to take 1·12 µm sections through cells expressing EGFP and ECFP tagged N proteins to visualize the nucleolus and the FC. Bright field microscopy (Fig. 2b) and the nucleolar markers (EGFP–nucleolin and DS-red-B23) (Fig. 2c and d, respectively) indicated that the FC was present in cells expressing ECFP–SARS-CoV-N. These markers also showed that there was no difference in the distribution of EGFP–nucleolin and DS-red-B23 between mock-transfected cells and those cells expressing ECFP–SARS-CoV-N. The data indicated that whilst EGFP–fibrillarin was punctate in appearance in untreated cells (Fig. 2a), it appeared more evenly distributed in the DFC in cells co-expressing ECFP–SARS-CoV-N and EGFP–fibrillarin (Fig. 2e). Redistribution and/or interaction with fibrillarin has been described previously for both coronavirus and arterivirus N proteins (Chen *et al.*, 2002; Yoo *et al.*, 2003).

Trafficking of proteins to the nucleus can be directed by appropriate nuclear localization signals (NLSs) including pat4, pat7 and bipartite motifs, which are groupings of arginine and lysine residues (Macara, 2001). Export of proteins from the nucleus is mediated via nuclear export signals (NESs) perhaps best characterized by CRM-1-dependent signals, which share a leucine-rich motif (Macara, 2001; Ossareh-Nazari *et al.*, 2001). In contrast, nucleolar retention/localization signals (NoRSs/NoLSs) are not well characterized and there is no consensus sequence (Carmona-Fonseca *et al.*, 2000). Marra *et al.* (2003) suggested that SARS-CoV-N contained a pat7 NLS in region III located between amino acid residues 369 and 376, and predicted that potential nuclear localization of SARS-CoV-N could account for the unique pathogenesis of the virus compared with other coronaviruses. However, coronaviruses representative of three known groups also contain potential NLSs in region III (Hiscox *et al.*, 2001; Wurm *et al.*, 2001), indeed the pat7 motif identified in SARS-CoV-N is most similar to the pat7 motif located in region III of IBV-N. Using bioinformatic analysis (la Cour *et al.*, 2004; Nakai & Horton, 1999), we found that SARS-CoV-N contained both pat7 and pat4, and bipartite NLSs, as well as a potential CRM-1-dependent NES (Fig. 3a). In contrast, IBV-N contained two overlapping pat4 and pat7 motifs and a potential CRM-1-dependent NES in region III (data not shown). A number of cellular and viral proteins have multiple NLSs, which regulate their nuclear localization (Burich & Lei, 2003; Haffar *et al.*, 2000; Luo *et al.*, 2004; Stelz *et al.*, 2002; Tsai & McKay, 2005), and therefore we predicted that SARS-CoV-N may contain signals that modulate its localization.

We hypothesized that SARS-CoV-N regions I (aa 1–156) and III (aa 300–422) would direct nuclear localization, with

region III being the most pronounced as it had three potential NLSs, and region II (aa 157–299) exhibiting nuclear and possibly cytoplasmic localization, as this region also contains a potential NES motif (Fig. 3a). To test this hypothesis, we cloned the regions downstream of ECFP, creating pECFP-SARS-CoV-RI, pECFP-SARS-CoV-RII and pECFP-SARS-CoV-RIII, whose expression would lead to the synthesis of ECFP tagged to SARS-CoV-N regions I, II and III, respectively. The proteins were visualized using live-cell and fixed imaging, and to visualize nucleoli proteins were imaged by confocal microscopy and staining with propidium iodide (Fig. 3b). ECFP–SARS-CoV-RI localized predominately to the nucleus with some cytoplasmic localization, but not to the nucleolus. ECFP–SARS-CoV-RII localized predominately to nucleoli and ECFP–SARS-CoV-RIII localized to the cytoplasm, cytoplasm and nucleus, and cytoplasm and nucleoli. The most frequent being cytoplasmic localization. Although these fragments contain predicted NLSs, alternatively nuclear/nucleolar localization of these proteins could be directed by their interaction with other cellular proteins, which contain appropriate NLSs/NoRSs. For example, nucleolar targeting of hepatitis δ -antigen is mediated through binding to nucleolin (Lee *et al.*, 1998).

Given that SARS-CoV-N region II contains a predicted NES, but was retained in the nucleolus, we examined the potential of this motif to direct nuclear export of EGFP. Aa 220–240, encompassing the predicted NES, were cloned downstream of EGFP. Expression of this plasmid in transfected cells indicated that EGFP–NES was non-functional (Fig. 3c) and had a similar localization pattern to EGFP (Fig. 1d). Given that SARS-CoV-N contains at least five potential NLSs, we would have predicted that deletion of aa 228–234 (encompassing the predicted NES) in the full-length SARS-CoV-N would have resulted in ECFP–SARS-CoV-N being localized to the nucleus. However, ECFP–SARS-CoV-N with the NES deletion (ECFP–N- Δ NES) remained localized to the cytoplasm (Fig. 3d), suggesting the presence of an alternative nuclear export/cytoplasmic retention signal.

Therefore, we tested the ability of the potential double pat7/bipartite nuclear localization located in region III to direct ECFP to the nucleus and found that localization of this protein was entirely nuclear (Fig. 3e) compared with ECFP alone (Fig. 1c), indicating that this motif was a functional NLS. Given that ECFP–SARS-CoV-RIII localized to the cytoplasm, this region may therefore contain a dominant cytoplasmic retention/nuclear export signal that acts on the whole protein. Certainly, treatment of cells expressing ECFP–SARS-CoV-N with 8 ng leptomycin B (Sigma-Aldrich) ml⁻¹ did not reveal any retention of ECFP–SARS-CoV-N in the nucleus (data not shown), unlike similar experiments with an arterivirus N protein (Tijms *et al.*, 2002).

Our data indicates that overexpressed SARS-CoV-N can localize to the cytoplasm and nucleolus, but with significantly less efficiency than IBV-N. No nucleolar localization

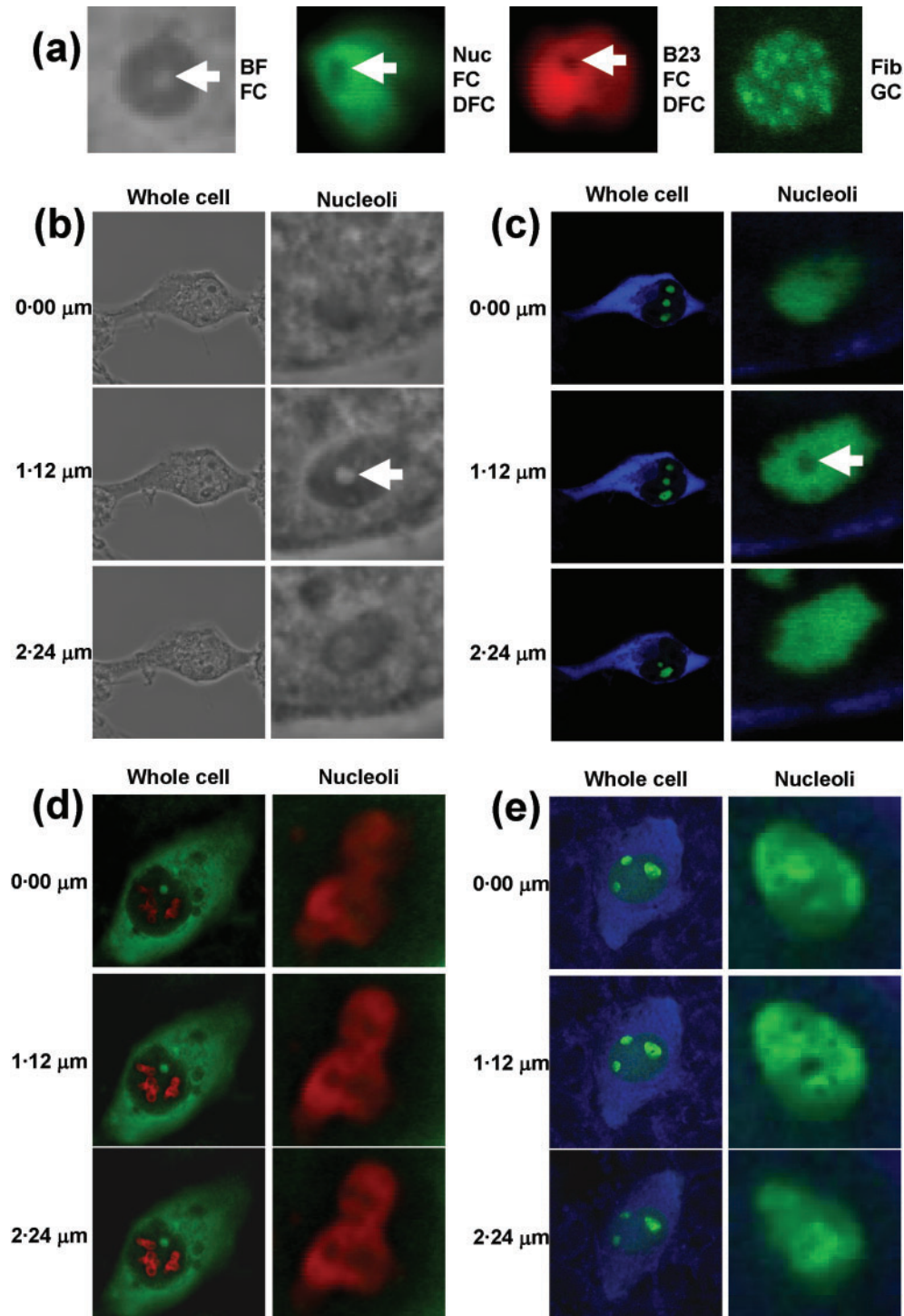


Fig. 2. (a) Markers for different regions of the nucleolus. Bright field (BF) microscopy for the FC, EGFP-nucleolin (Nuc), DS-red-B23 (B23) for the FC and DFC, and EGFP-fibrillarin (Fib) for the GC. Cells expressing ECFP-SARS-CoV-N examined by BF microscopy (b) and confocal microscopy using selected fluorescent tagged markers, EGFP-nucleolin (c), DS-red-B23 (d) and EGFP-fibrillarin (e) to visualize distinct regions of the nucleolus. Optical sections (shown as 1.12 μm increments) were taken to visualize the FC (arrows). Nucleoli are electronically enhanced.

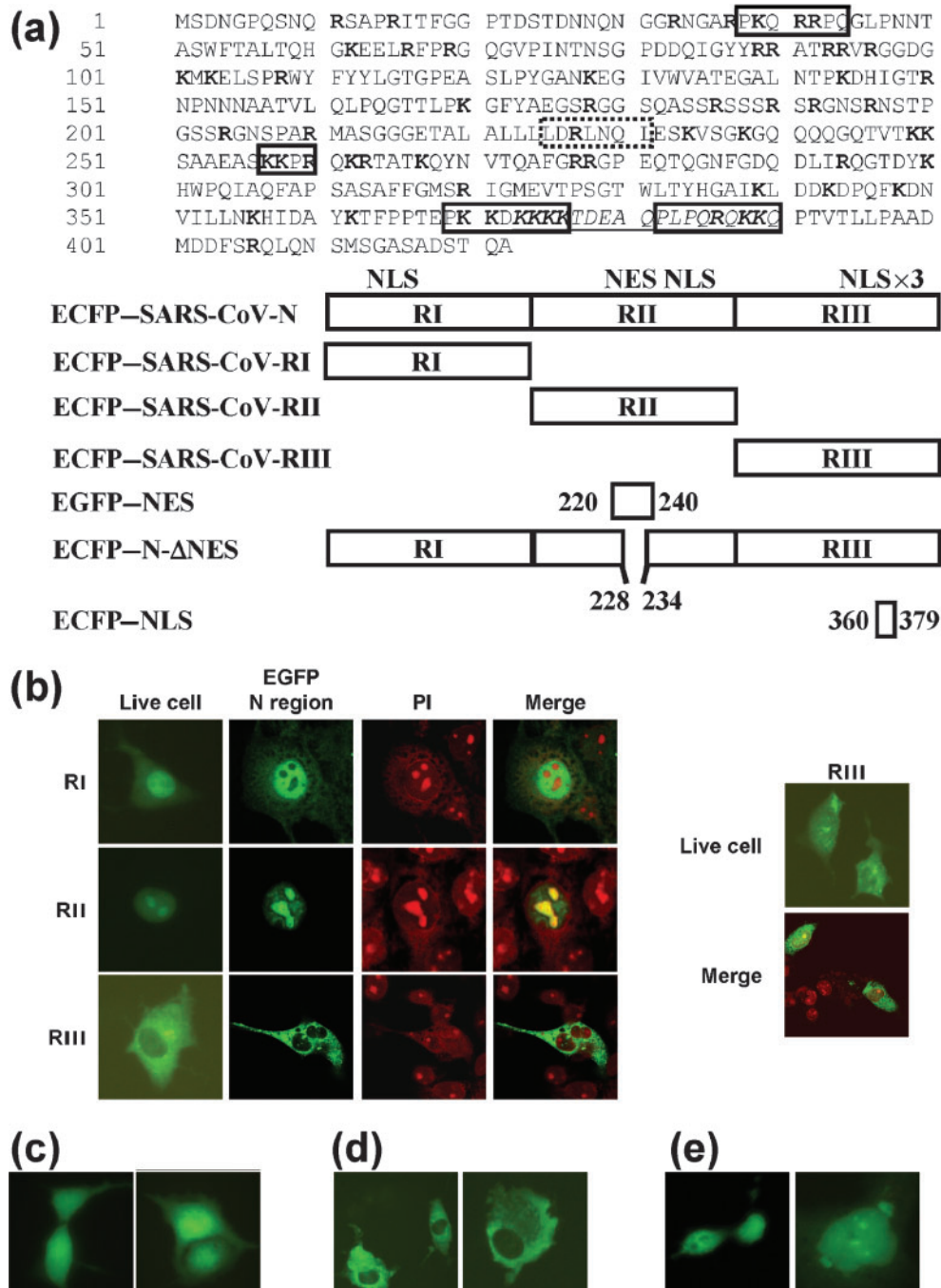


Fig. 3. (a) Amino acid sequence of the SARS-CoV-N with potential pat4 and pat7 NLSs boxed, the potential bipartite NLS is underlined and the potential NES is outlined by the hashed box, arginine and lysine residues are shown in bold face, and a putative bipartite NLS is shown in italics. Below this are schematic representations of the constructs used to investigate the distribution of localization signals in the SARS-CoV-N. All constructs were sequenced and their expression confirmed by Western blot (data not shown). (b) Live-cell and confocal images (individual channel plus merged), showing the distribution of ECFP-SARS-CoV-RI, ECFP-SARS-CoV-RII and ECFP-SARS-CoV-RIII (several examples of which are given). PI, Propidium iodide. Live-cell images of EGFP-NES (c), ECFP-N-ΔNES (d) and ECFP-NLS (e) are shown.

of SARS-CoV-N was observed in virus-infected cells, and the difference between this and overexpression maybe due to a number of factors including the ability of antibodies to penetrate the nucleolus, association of N protein with other viral proteins or modification of the protein. The data suggests that region II contains a NoRS, and that whilst regions I and III contain NLSs, in the case of region III this is overridden by an undefined non-CRM-1 NES/cytoplasmic retention motif, which may be the dominant signal for localization of SARS-CoV-N inside the cell. Conformational change of the protein, perhaps through differential phosphorylation or cleavage, may expose the NLSs/NoRS with low efficiency.

Acknowledgements

This work was in part funded by the BBSRC (grant number BBS/B/03416) to J.A.H. The confocal microscope facility in the Astbury Centre for Structural Molecular Biology was funded by the Wellcome Trust. M. Z. acknowledges funding from the Health Protection Agency. The HKU 39849 strain of SARS-CoV was kindly provided by Malik Peiris. L. E. acknowledges funding from the Ministry of Education and Science of Spain and EU Project 'Biosafe Vaccine Vector' grant number QLRI-2000-00874.

References

- Andersen, J. S., Lam, Y. W., Leung, A. K., Ong, S. E., Lyon, C. E., Lamond, A. I. & Mann, M. (2005). Nucleolar proteome dynamics. *Nature* **433**, 77–83.
- Burich, R. & Lei, M. (2003). Two bipartite NLSs mediate constitutive nuclear localization of Mcm10. *Curr Genet* **44**, 195–201.
- Calvo, E., Escors, D., Lopez, J. A., Gonzalez, J. M., Alvarez, A., Arza, E. & Enjuanes, L. (2005). Phosphorylation and subcellular localization of transmissible gastroenteritis virus nucleocapsid protein in infected cells. *J Gen Virol* **86**, 2255–2267.
- Carmo-Fonseca, M., Mendes-Soares, L. & Campos, I. (2000). To be or not to be in the nucleolus. *Nat Cell Biol* **2**, E107–E112.
- Chen, H., Wurm, T., Britton, P., Brooks, G. & Hiscox, J. A. (2002). Interaction of the coronavirus nucleoprotein with nucleolar antigens and the host cell. *J Virol* **76**, 5233–5250.
- Chen, H., Gill, A., Dove, B. K., Emmett, S. R., Kemp, F. C., Ritchie, M. A., Dee, M. & Hiscox, J. A. (2005). Mass spectroscopic characterisation of the coronavirus infectious bronchitis virus nucleoprotein and elucidation of the role of phosphorylation in RNA binding using surface plasmon resonance. *J Virol* **79**, 1164–1179.
- Gustin, K. E. (2003). Inhibition of nucleo-cytoplasmic trafficking by RNA viruses: targeting the nuclear pore complex. *Virus Res* **95**, 35–44.
- Gustin, K. E. & Sarnow, P. (2001). Effects of poliovirus infection on nucleo-cytoplasmic trafficking and nuclear pore complex formation. *EMBO J* **20**, 240–249.
- Gustin, K. E. & Sarnow, P. (2002). Inhibition of nuclear import and alteration of nuclear pore complex composition by rhinovirus. *J Virol* **76**, 8787–8796.
- Haffar, O. K., Popov, S., Dubrovsky, L., Agostini, I., Tang, H., Pushkarsky, T., Nadler, S. G. & Bukrinsky, M. (2000). Two nuclear localization signals in the HIV-1 matrix protein regulate nuclear import of the HIV-1 pre-integration complex. *J Mol Biol* **299**, 359–368.
- He, R., Leeson, A., Andonov, A. & 8 other authors (2003). Activation of AP-1 signal transduction pathway by SARS coronavirus nucleocapsid protein. *Biochem Biophys Res Commun* **311**, 870–876.
- Hiscox, J. A. (2002). Brief review: the nucleolus – a gateway to viral infection? *Arch Virol* **147**, 1077–1089.
- Hiscox, J. A. (2003). The interaction of animal cytoplasmic RNA viruses with the nucleus to facilitate replication. *Virus Res* **95**, 13–22.
- Hiscox, J. A., Wurm, T., Wilson, L., Cavanagh, D., Britton, P. & Brooks, G. (2001). The coronavirus infectious bronchitis virus nucleoprotein localizes to the nucleolus. *J Virol* **75**, 506–512.
- Jayaram, J., Youn, S. & Collisson, E. W. (2005). The virion N protein of infectious bronchitis virus is more phosphorylated than the N protein from infected cell lysates. *Virology* **339**, 127–135.
- la Cour, T., Kiemer, L., Molgaard, A., Gupta, R., Skriver, K. & Brunak, S. (2004). Analysis and prediction of leucine-rich nuclear export signals. *Protein Eng Des Sel* **17**, 527–536.
- Lam, Y. W., Trinkle-Mulcahy, L. & Lamond, A. I. (2005). The nucleolus. *J Cell Sci* **118**, 1335–1337.
- Lee, C. H., Chang, S. C., Chen, C. J. & Chang, M. F. (1998). The nucleolin binding activity of hepatitis delta antigen is associated with nucleolus targeting. *J Biol Chem* **273**, 7650–7656.
- Lundberg, M. & Johansson, M. (2001). Is VP22 nuclear homing an artifact? *Nat Biotechnol* **19**, 713.
- Lundberg, M. & Johansson, M. (2002). Positively charged DNA-binding proteins cause apparent cell membrane translocation. *Biochem Biophys Res Commun* **291**, 367–371.
- Luo, M., Pang, C. W., Gerken, A. E. & Brock, T. G. (2004). Multiple nuclear localization sequences allow modulation of 5-lipoxygenase nuclear import. *Traffic* **5**, 847–854.
- Luo, H., Chen, Q., Chen, J., Chen, K., Shen, X. & Jiang, H. (2005). The nucleocapsid protein of SARS coronavirus has a high binding affinity to the human cellular heterogeneous nuclear ribonucleoprotein A1. *FEBS Lett* **579**, 2623–2628.
- Macara, I. G. (2001). Transport into and out of the nucleus. *Microbiol Mol Biol Rev* **65**, 570–594.
- Marra, M. A., Jones, S. J. M. & Astell, C. R. (2003). The genome sequence of the SARS-associated coronavirus. *Science* **300**, 1399–1404.
- Nakai, K. & Horton, P. (1999). PSORT: a program for detecting sorting signals in proteins and predicting their subcellular localization. *Trends Biochem Sci* **24**, 34–36.
- Ning, Q., Lakatoo, S., Liu, M. F., Yang, W. M., Wang, Z. M., Phillips, M. J. & Levy, G. A. (2003). Induction of prothrombinase *fgl2* by the nucleocapsid protein of virulent mouse hepatitis virus is dependent on host hepatic nuclear factor-4 α . *J Biol Chem* **278**, 15541–15549.
- Ossareh-Nazari, B., Gwizdek, C. & Dargemont, C. (2001). Protein export from the nucleus. *Traffic* **2**, 684–689.
- Parker, M. M. & Masters, P. S. (1990). Sequence comparison of the N genes of five strains of the coronavirus mouse hepatitis-virus suggests a three domain-structure for the nucleocapsid protein. *Virology* **179**, 463–468.
- Qin, Z., Jinming, C., Xiaojun, H., Huanying, Z., Jicheng, H., Ling, F., Kunpeng, L. & Jingqiang, Z. (2004). The life cycle of SARS coronavirus in Vero E6 cells. *J Med Virol* **73**, 332–337.
- Risco, C., Anton, I. M., Enjuanes, L. & Carrascosa, J. L. (1996). The transmissible gastroenteritis coronavirus contains a spherical core shell consisting of M and N proteins. *J Virol* **70**, 4773–4777.
- Rowland, R. R., Kerwin, R., Kuckleburg, C., Sperlich, A. & Benfield, D. A. (1999). The localization of porcine reproductive and respiratory syndrome virus nucleocapsid protein to the nucleolus of infected cells and identification of a potential nucleolar localization signal sequence. *Virus Res* **64**, 1–12.

Sheval, E. V., Polzikov, M. A., Olson, M. O. & Zatsepina, O. V. (2005). A higher concentration of an antigen within the nucleolus may prevent its proper recognition by specific antibodies. *Eur J Histochem* **49**, 117–123.

Stelz, G., Rucker, E., Rosorius, O., Meyer, G., Stauber, R. H., Spatz, M., Eibl, M. M. & Hauber, J. (2002). Identification of two nuclear import signals in the α -gene product ICP22 of herpes simplex virus 1. *Virology* **295**, 360–370.

Surjit, M., Liu, B., Jameel, S., Chow, V. T. & Lal, S. K. (2004). The SARS coronavirus nucleocapsid protein induces actin reorganization and apoptosis in COS-1 cells in the absence of growth factors. *Biochem J* **383**, 13–18.

Thiry, M. & Lafontaine, D. L. (2005). Birth of a nucleolus: the evolution of nucleolar compartments. *Trends Cell Biol* **15**, 194–199.

Tijms, M. A., van der Meer, Y. & Snijder, E. J. (2002). Nuclear localization of non-structural protein 1 and nucleocapsid protein of equine arteritis virus. *J Gen Virol* **83**, 795–800.

Tsai, R. Y. L. & McKay, R. D. G. (2005). A multistep, GTP-driven mechanism controlling the dynamic cycling of nucleostemin. *J Cell Biol* **168**, 179–184.

Wurm, T., Chen, H., Hodgson, T., Britton, P., Brooks, G. & Hiscox, J. A. (2001). Localization to the nucleolus is a common feature of coronavirus nucleoproteins and the protein may disrupt host cell division. *J Virol* **75**, 9345–9356.

Yoo, D., Wootton, S. K., Li, G., Song, C. & Rowland, R. R. (2003). Colocalization and interaction of the porcine arterivirus nucleocapsid protein with the small nucleolar RNA-associated protein fibrillarin. *J Virol* **77**, 12173–12183.